From little whorls to the global atmosphere

Ulrich Schumann

37 years of personal nonlinear dynamics

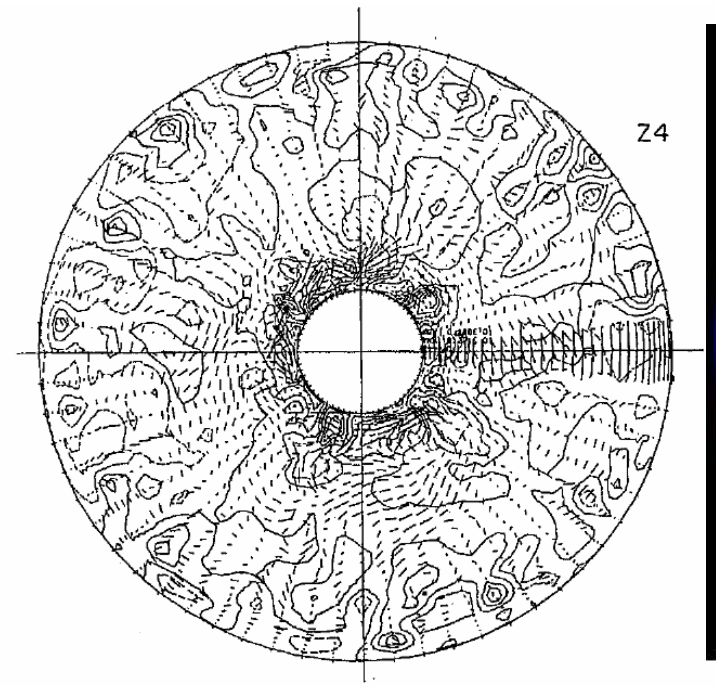

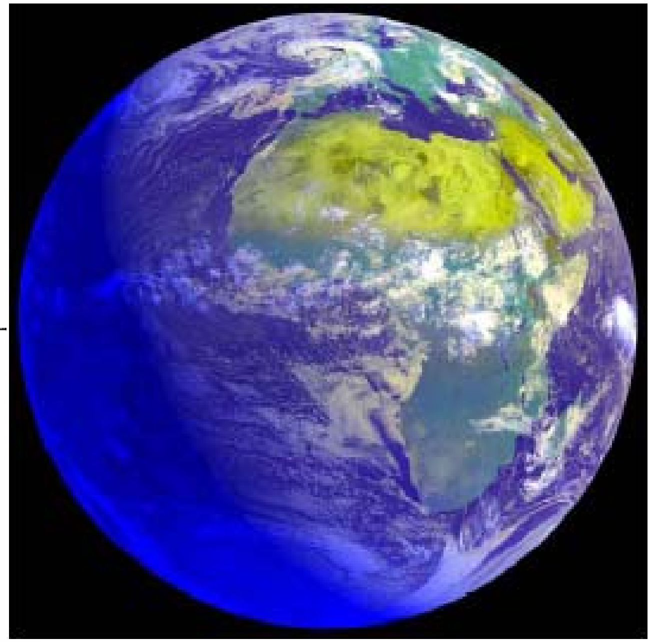

*"Dr. Richardson said
that the atmosphere resembled London -
for in both there were always
far more things going on
than anyone could properly attend to."*

Simpson (1929)

The Richardson cascade[1] (1922)

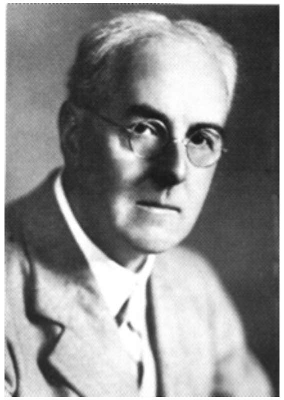

L. F. Richardson

(1881-1953)

Big whorls have little whorls,
that feed on their velocity,
and little whorls have lesser whorls,
and so on to viscosity

L. F. Richardson (1922)

$$K \sim r^{4/3}$$

Kolmogoroff (1941):

$$E(k) = \alpha\, \varepsilon^{2/3}\, k^{-5/3}$$

[1] Hunt (1993)

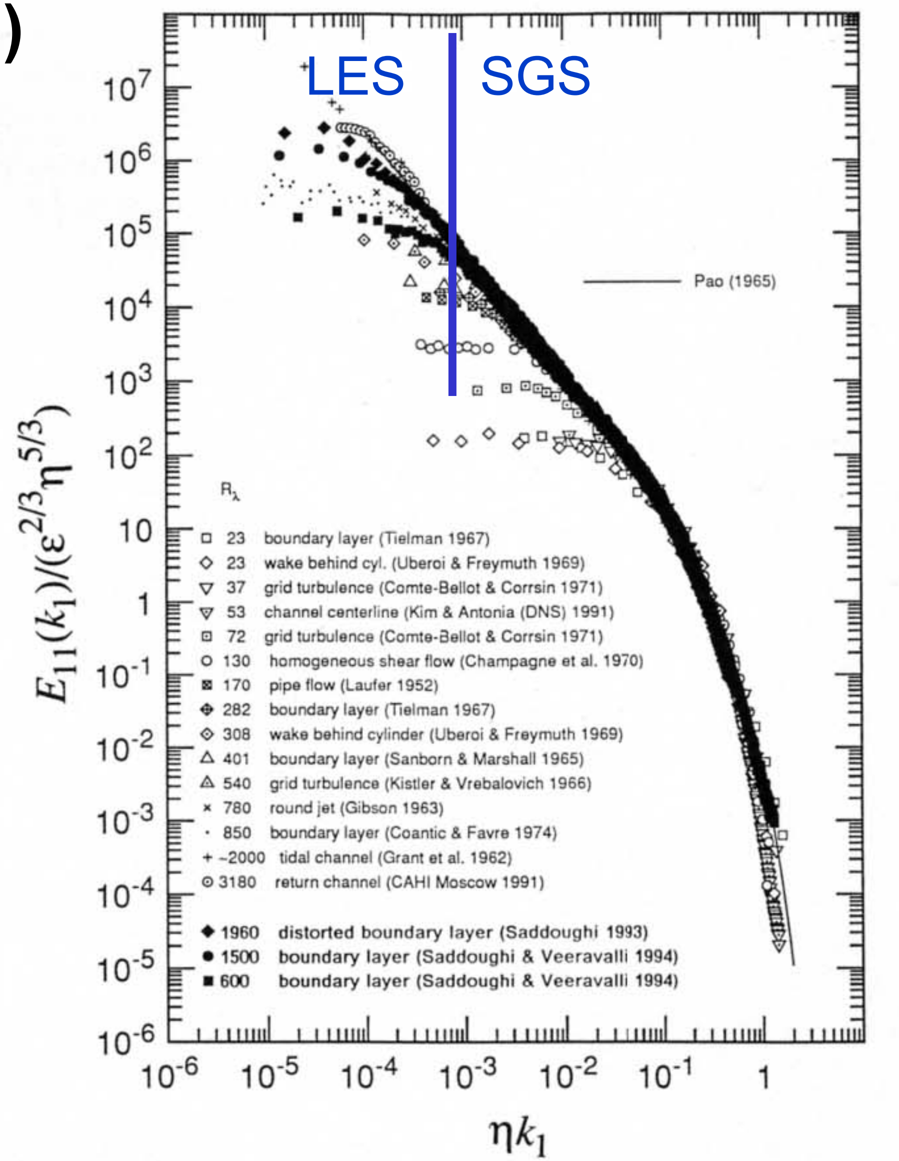

Figure 1 One-dimensional longitudinal energy spectra of turbulent flows at various Reynolds numbers R_λ in Kolmogorov's scales compared to Pao's (1965) spectral model, from Saddoughi and Veeravalli (1994) with additions from Saddoughi (1993). The graph has been kindly provided by S. G. Saddoughi.

SGS models for Δ in inertial sub-range

$e = \int_{k>\pi/\Delta} E(k)dk$, for $P = \varepsilon$

$$\varepsilon = \frac{e^{3/2}}{l_\varepsilon},$$

$$K_m = l_m e^{1/2}, \qquad K_h = K_c = l_h e^{1/2},$$

$$l_\varepsilon = \frac{l}{c_\varepsilon}, \qquad l_m = c_m l, \qquad l_h = c_h l,$$

$$l = \Delta,$$

$$c_\varepsilon = \left(\frac{2}{3\alpha}\right)^{3/2} \pi = 0.845,$$

$$c_m = \left(\frac{2}{3\alpha}\right)^{3/2} \frac{1}{\pi} = 0.0856,$$

$$c_h = \left(\frac{2}{3\alpha}\right)^{1/2} \frac{4}{3\gamma} \frac{1}{\pi} = 0.204,$$

(Lilly, 1967, Deardorff, 1972, Schumann, 1991)

LES: allows to save 8-16 orders of magnitude of computing time

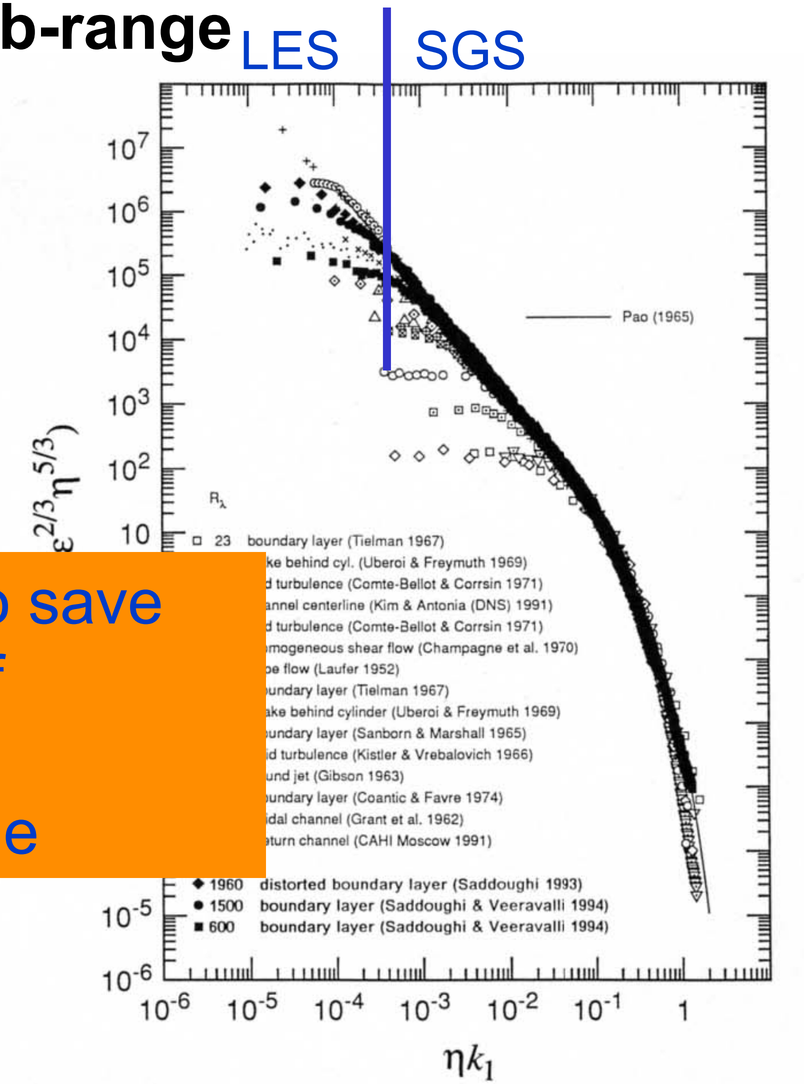

Figure 1 One-dimensional longitudinal energy spectra of turbulent flows at various Reynolds numbers R_λ in Kolmogorov's scales compared to Pao's (1965) spectral model, from Saddoughi and Veeravalli (1994) with additions from Saddoughi (1993). The graph has been kindly provided by S. G. Saddoughi.

10 July 1973:

Dieter Smidt with 3 of his Doctorands

J. Fluid Mech. (1970), *vol.* 41, *part* 2, *pp.* 453–480
Boeing Symposium on Turbulence

first successful "LES"

A numerical study of three-dimensional turbulent channel flow at large Reynolds numbers

By JAMES W. DEARDORFF
National Center for Atmospheric Research, Boulder, Colorado 80302

$$\overline{u_i' u_j'} - \tfrac{1}{3}\delta_{ij}\,\overline{u_l' u_l'} = -K\left(\frac{\partial \overline{u}_i}{\partial x_j} + \frac{\partial \overline{u}_j}{\partial x_i}\right)$$

$$\Delta = (\Delta x \,.\, \Delta y \,.\, \Delta z)^{\frac{1}{3}}.$$

$$K(x,y,z,t) = (c\Delta)^2\left[\frac{\partial \overline{u}_i}{\partial x_j}\left(\frac{\partial \overline{u}_i}{\partial x_j} + \frac{\partial \overline{u}_j}{\partial x_i}\right)\right]^{\frac{1}{2}}$$

$c \simeq 0{\cdot}17$ Smagorinsky et al., (1965)

$c = 0{\cdot}10$ Lilly (1967)

24 x 14 x 20 grid cells

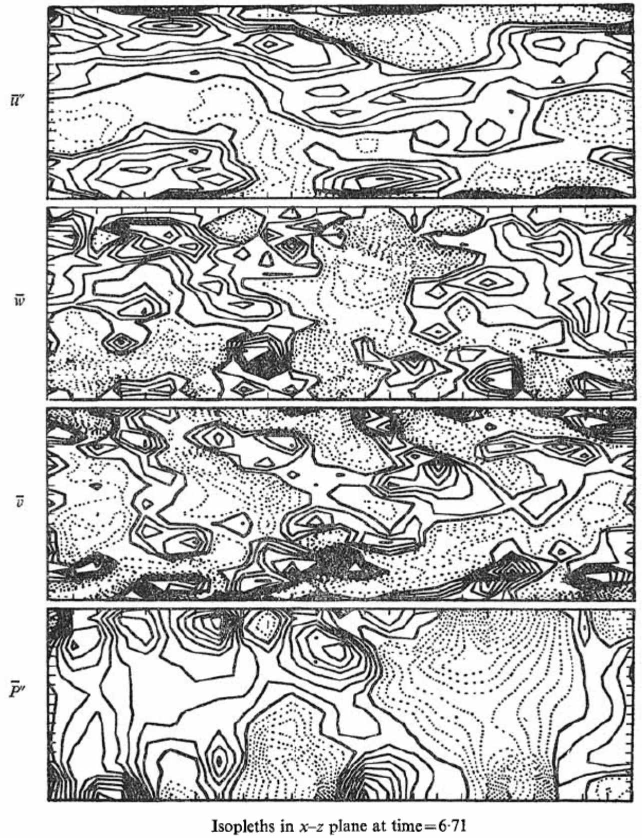

FIGURE 2. Contours of velocity components $\overline{u}''$, $\overline{w}$, $\overline{v}$ and of pressure $\overline{P}''$ in an x–z plane.

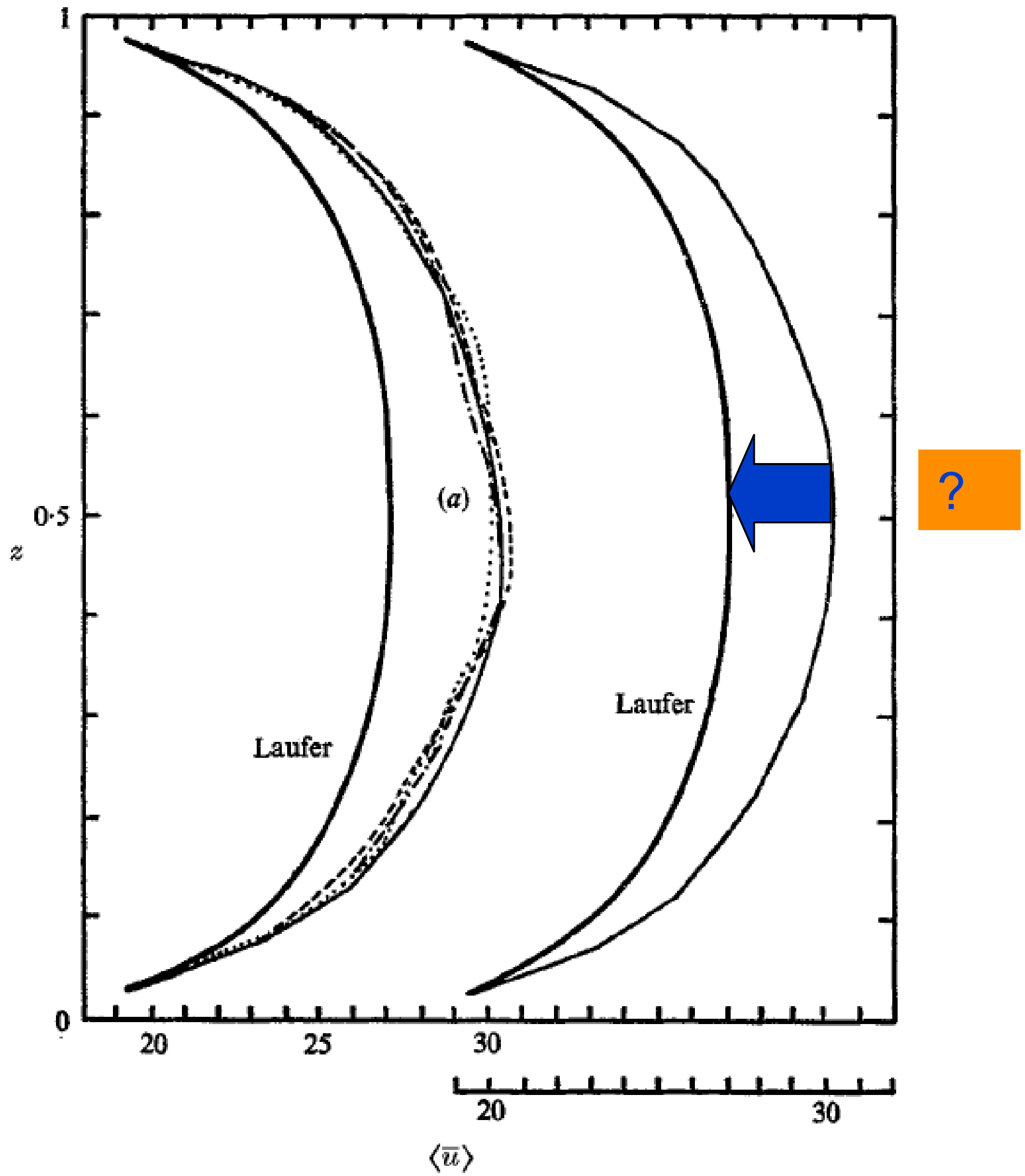

Deardorff (1970)

FIGURE 1. Calculated and measured mean wind profiles (made dimensionless by u^*). Thin curves in (a) were calculated at four widely separated times between $t = 0$ and $t = 7{\cdot}41$. Thin curve in (b) is the average of 10 such profiles. Heavy curve is from Laufer (1950).

Numerical simulation of three-dimensional turbulent flow in a ring channel

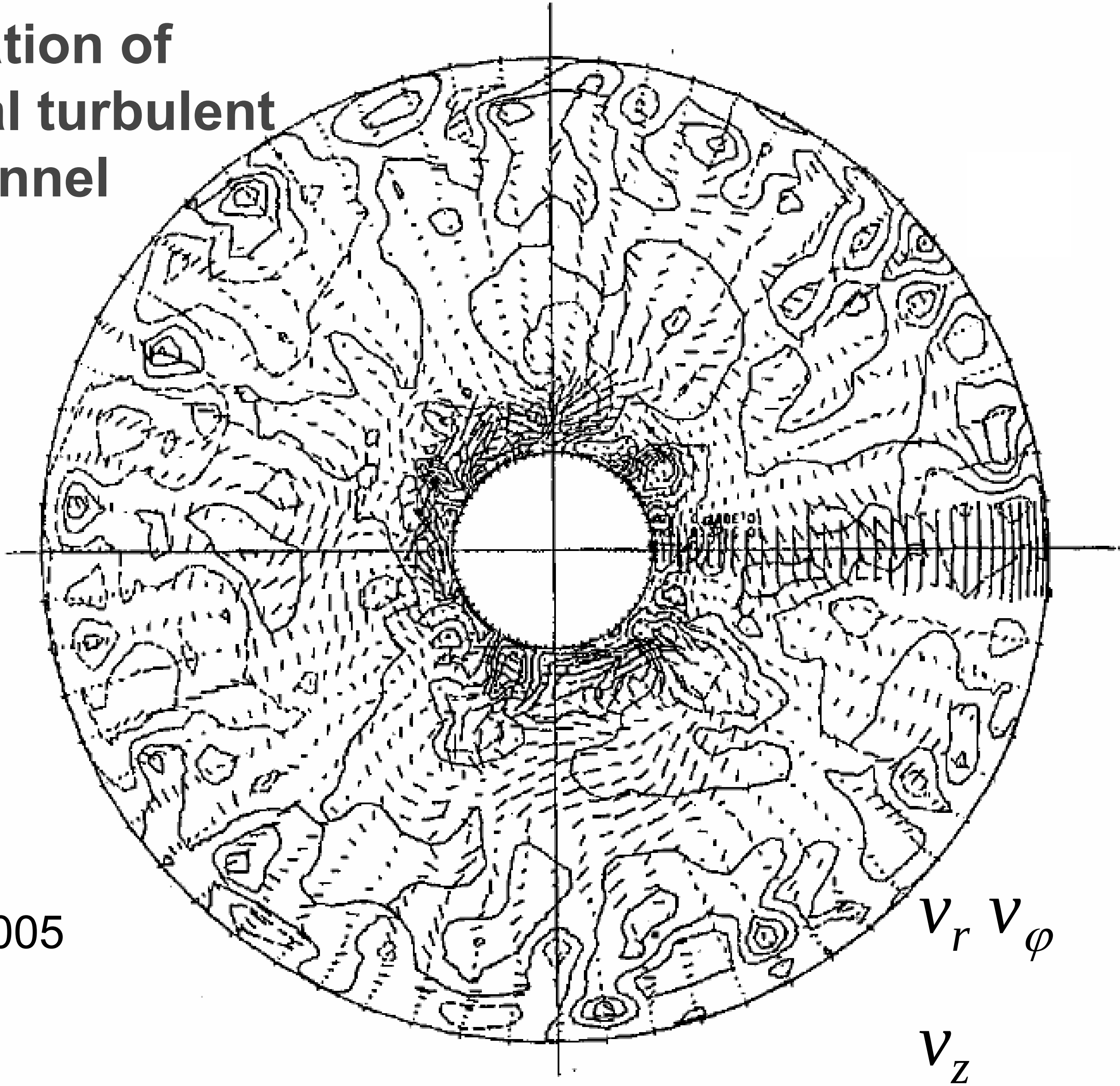

variable degree of cell size and anisotropy

(Schumann, JCP, 2005

64 x 64 x 32)

v_r v_φ

v_z 。

Filtering defined by grid and finite difference operators

$${}^{V}\overline{y} \equiv \frac{1}{\Delta x_1\, \Delta x_2\, \Delta x_3} \int_{\Delta x_1} \int_{\Delta x_2} \int_{\Delta x_3} y(z_1\,,\, z_2$$

$${}^{1}\overline{y} \equiv \frac{1}{\Delta x_2\, \Delta x_3} \int_{\Delta x_2} \int_{\Delta x_3} y(x_1\,,\, z_2\,,\, z_3)\, dz_2\, dz_3$$

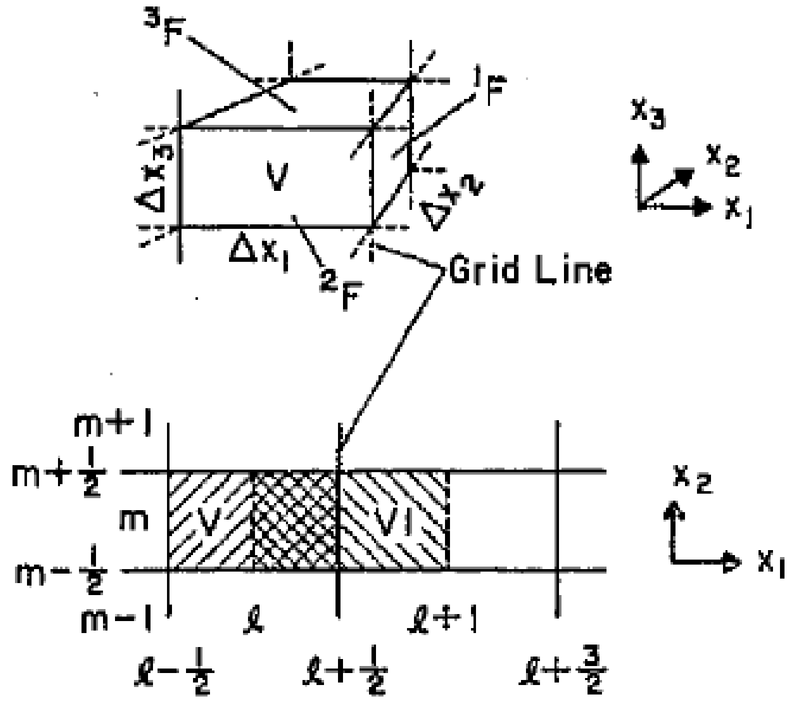

FIG. 2. Grid volumes and surfaces.

$${}^{V1}\overline{\frac{Du_i}{Dt}} = \frac{\partial}{\partial t}\, {}^{V1}\overline{u_i} + \delta_j\left({}^{j}\overline{u_j}\; {}^{j}\overline{u_i}\right) = -\delta_i\, {}^{i}\overline{p} + \delta_j \left(\nu\, {}^{j}\overline{\frac{\partial u_i}{\partial x_j}} - {}^{j}\overline{u_i' u_j'} \right) + P_\omega\, \delta_{1i}$$

$${}^{j}\overline{u_i' u_j'} \equiv {}^{j}\overline{(u_i - {}^{j}\overline{u_i})(u_j - {}^{j}\overline{u_j})} = {}^{j}\overline{u_i u_j} - {}^{j}\overline{u_i}\; {}^{j}\overline{u_j}$$

(Schumann, JCP, 2005)

Subgrid-scale model: a two-part SGS model (Schumann, 1975)

$$ {}^{j}\overline{u_i' u_j'} = -\underbrace{{}^{ij}\mu(\overline{D}_{ij} - \langle \overline{D}_{ij} \rangle)}_{\text{"locally isotropic part"}} \underbrace{- {}^{ij}\mu^* \langle \overline{D}_{ij} \rangle}_{\text{"inhomogeneous part"}} + \tfrac{1}{3}\delta_{ij}\ {}^{k}\overline{u_k' u_k'}. $$

$$ {}^{ij}\mu = c_2 ({}^{j}F\ {}^{j}\overline{E'})^{1/2}\ {}^{ij}c. $$

$$ {}^{13}\mu^* = ({}^{3}L)^2 \mid \delta_3 \langle u_i \rangle \mid $$

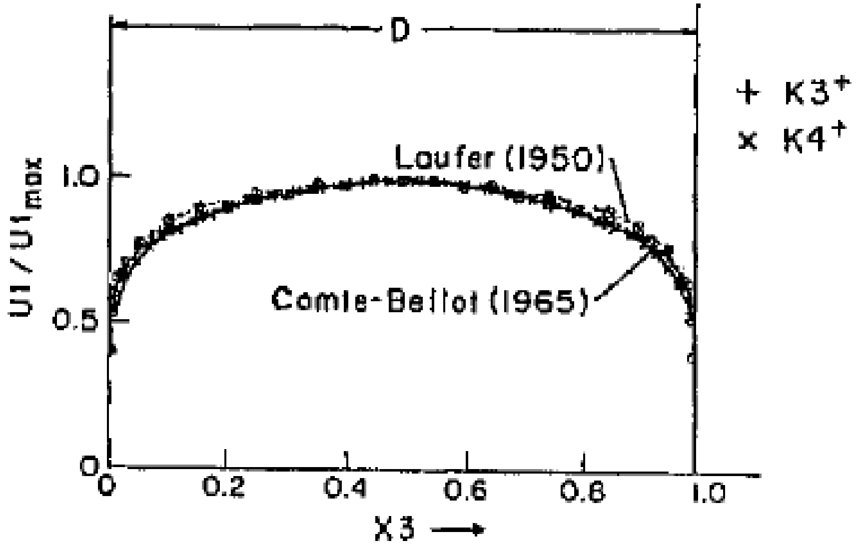

$$ \frac{\partial}{\partial t}\ {}^{\nu}\overline{E'} + \underbrace{\delta_j({}^{j}\overline{u_j}\ {}^{j}\overline{E'})}_{\text{convection}} = -\underbrace{\overline{{}^{j}\overline{u_i' u_j'}}^{\,j}\ \delta_j\ {}^{j}\overline{u_i}}_{\text{production}} - \underbrace{{}^{\nu}\overline{\epsilon}}_{\text{dissipation}} + \nu\underbrace{\{(\delta_j\ {}^{j}\overline{u_i})(\delta_j\ {}^{j}\overline{u_i} + \delta_i\ {}^{j}\overline{u_j})\}}_{\text{viscous gross scale dissipation}} + \underbrace{\delta_j \left\{ \nu\ {}^{j}\overline{\frac{\partial E'}{\partial x_j}} + {}^{j}\overline{u_i \frac{\partial u_j}{\partial x_i}} - {}^{j}\overline{u_i}\ {}^{j}\overline{\frac{\partial u_j}{\partial x_i}} - {}^{j}\overline{u_j' E'} - {}^{j}\overline{u_j' p'} \right\}}_{\text{diffusion}}. $$

Two part model: Sullivan, Williams & Moeng (BLM, 1994)

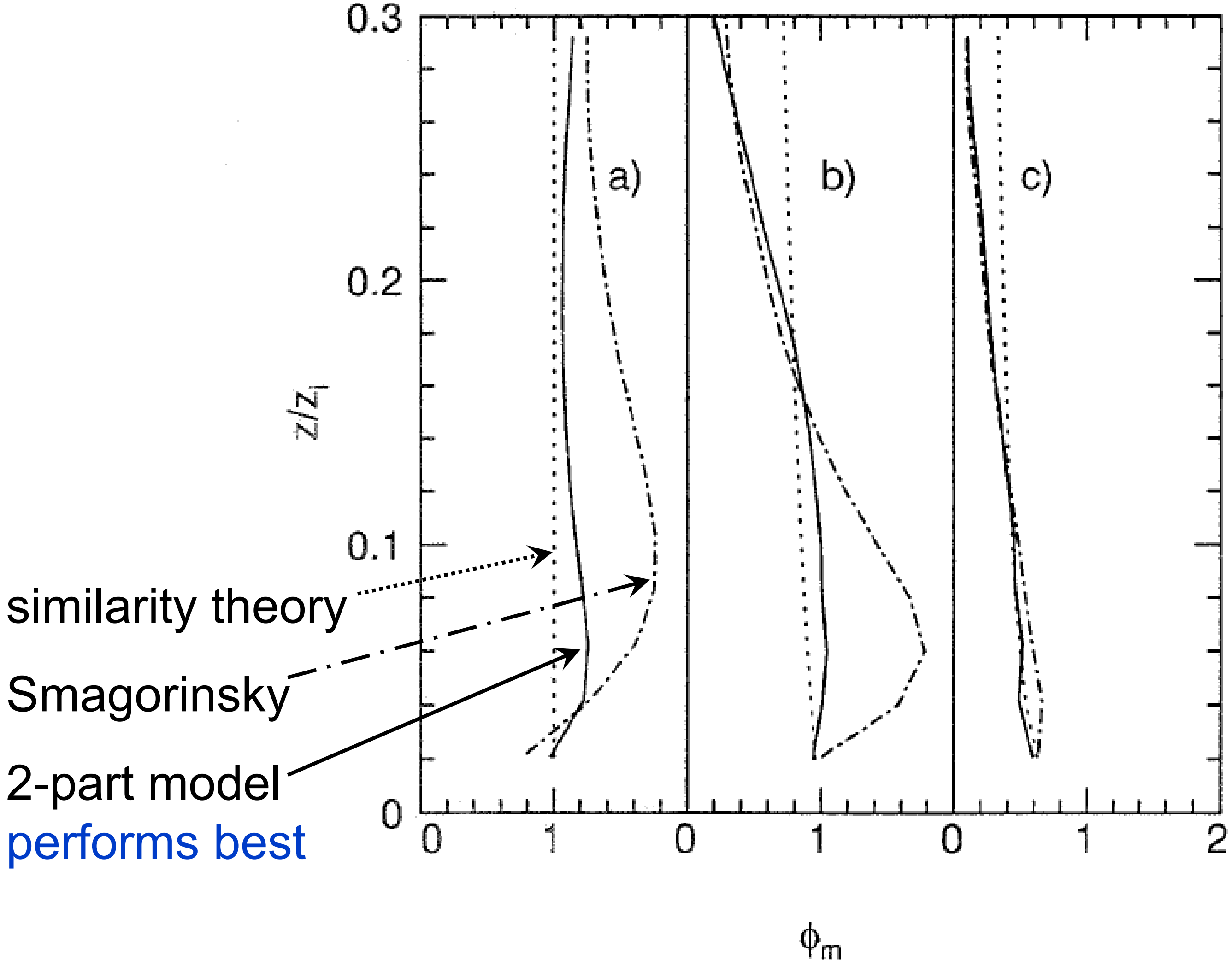

Fig. 2. Momentum stability function profiles; dotted line similarity theory, dashed-dot line baseline model, solid line new model; for the same flows as in Figure 1.

$$\frac{\partial U_s}{\partial z} = \frac{u_* \phi_m}{\kappa z}$$

a: neutral, b;: slightly, c: strongly convective

Realizability of Reynolds Stress Model

The Reynolds stresses are realizable

$R_{ij} = \langle u_i u_j \rangle$

- $x_i R_{ij} x_j = \langle x_i u_i u_j x_j \rangle \geq 0$
- autocorrelations $R_{11} \geq 0$,

  cross correlation $(R_{12})^2 \leq R_{11} R_{22}$
- $\lambda_i \geq 0$, i=1,2,3
- $I = R_{ii} \geq 0$,

  $II = (R_{ii} R_{jj} - R_{ij}^2) \geq 0$,

  $III = \det(R_{ij}) \geq 0$

Reynolds-Stress closure models should guarantee Realizability.

$dF/dt \geq 0$ in case $F = 0$

(Schumann, Phys. Fluids, 1977)

e.g., F = III

weak realizability

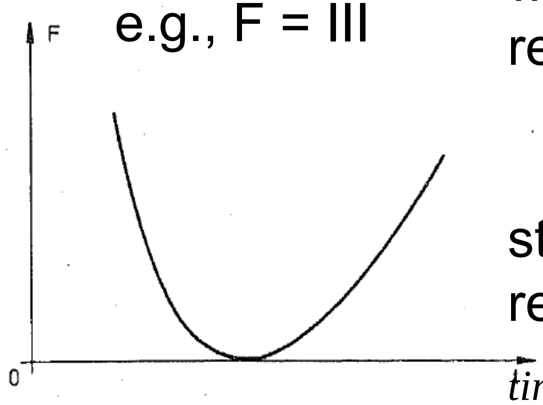

strong realizability

time

Required behaviour of F as a function of time t when approaching the limit F=0. F stands for one of the invariants.

Example. The following model

$$\Phi_{ij} = -c_1 \epsilon (R_{ij} - \delta_{ij} R_{kk}/3)/E \,,$$

$$\epsilon \equiv \epsilon_{kk}/2 \,, \qquad E \equiv R_{kk}/2 \,.$$

$$\epsilon_{ij} = 2\epsilon\left[d R_{ij}/R_{kk} + (1-d)\delta_{ij}/3 \right]$$

is realisable only for $c_1 \geq 1 - d$

Multiply the sources terms with a strong function of F, e.g. $1-(1-y)^A$, $y = III/(I/3)^3$

Implications for second-order closure models

- Lumley (1978): realizable turbulent state lies within the invariant triangle
- Shie and Lumley (1993)
- Speziale, Abib and Durbin (1994)
- Grimaji (JFM, 2004)

The closure for each of the unclosed statistical moments in the Reynolds stress equation must be individually realizable (Grimiaji, JFM, 2004)

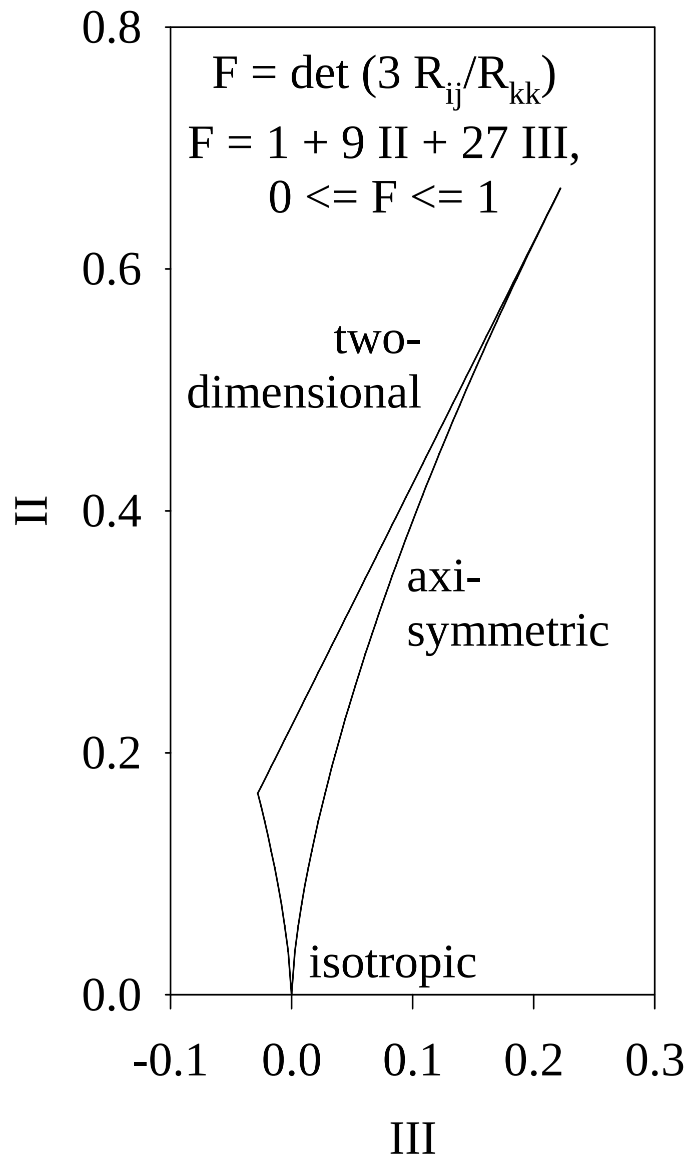

Large Eddy Simulation (LES) of the Convective Boundary Layer (CBL)

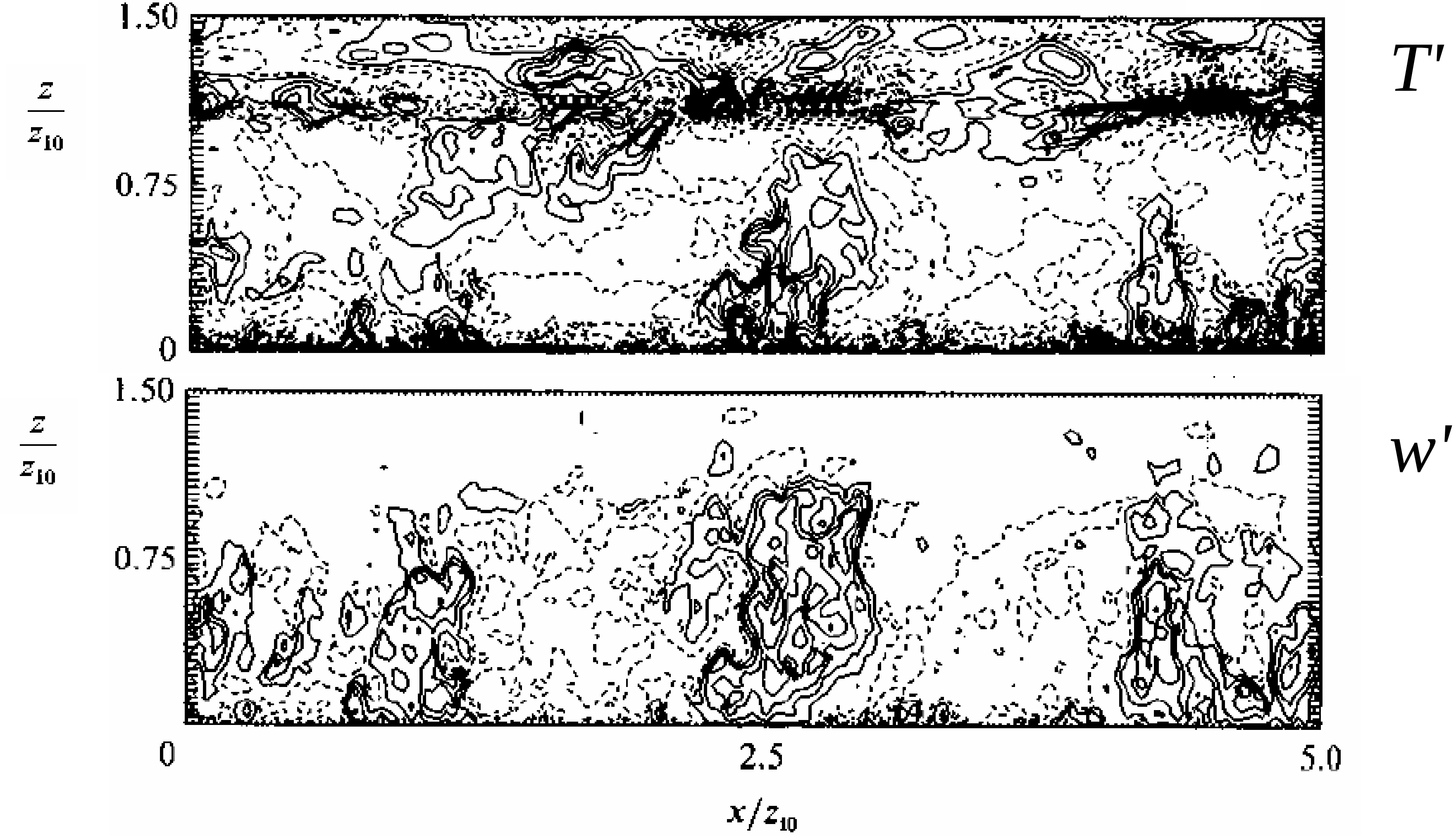

(Schmidt and Schumann, JFM, 1989)

Large Eddy Simulation (LES) of the Convective Boundary Layer (CBL)

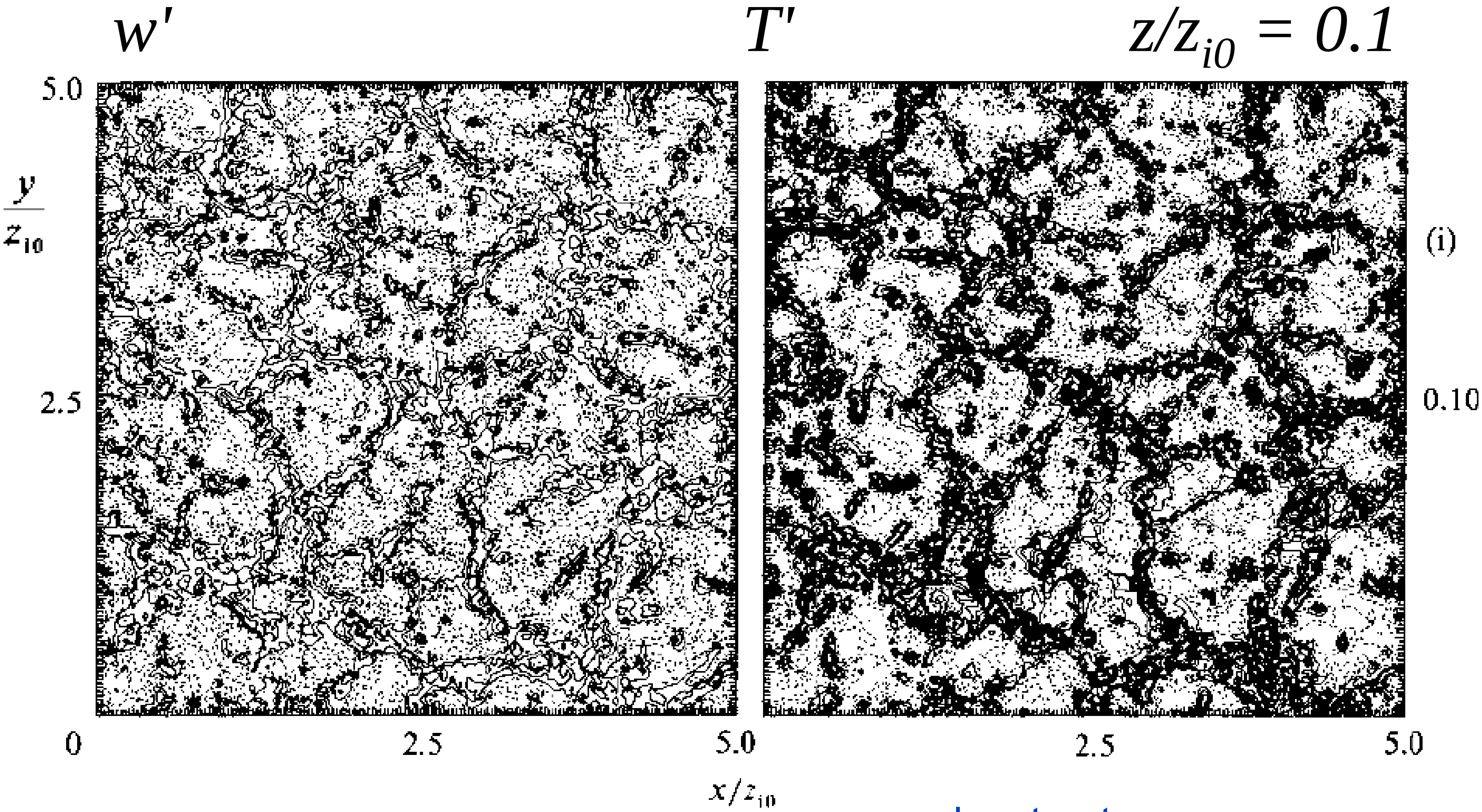

spoke structure

(Schmidt and Schumann, JFM, 1989)

Convective turbulence is easy to simulate with coarse LES

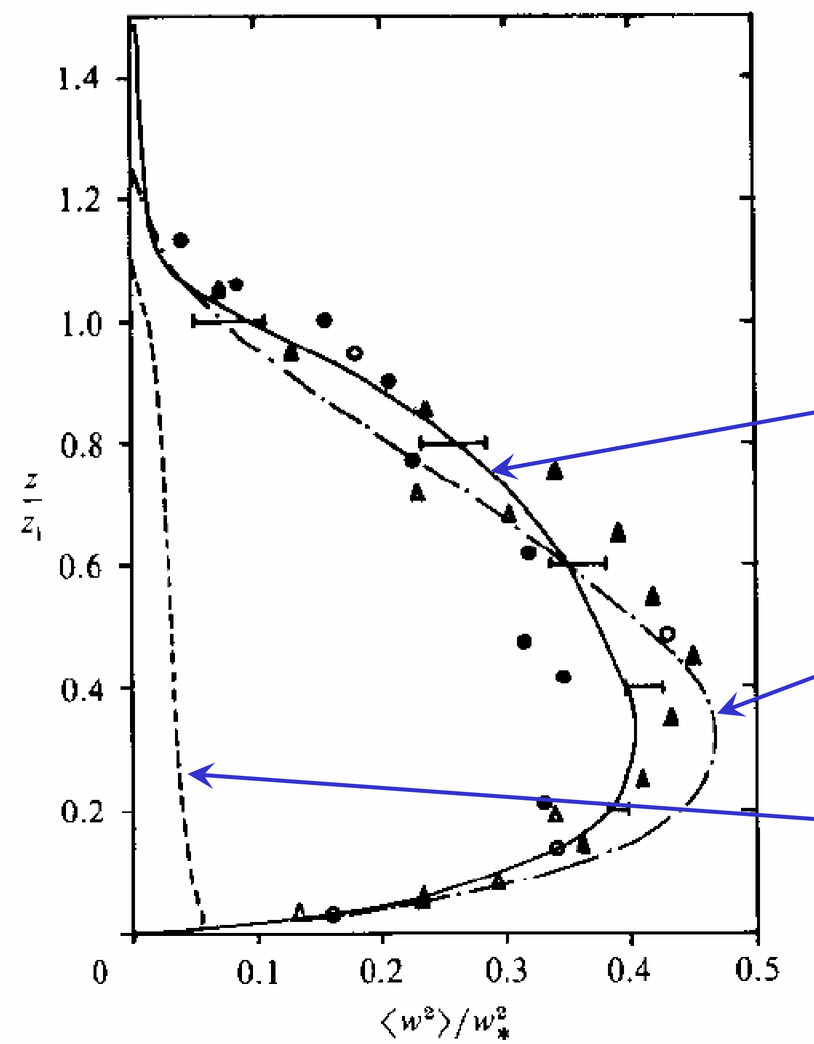

LES

compared to field and laboratory data

Lenschow (1980) scaling approximation

SGS

Schmidt & Schumann (JFM, 1989)

Backscatter

However, the transfer of energy does not follow a one-way street. Some energy gets backscattered from small to large scales.

Important if much energy at SGS (e.g. for coarse resolution and in global geophysical models)

<u>Common assumption:</u>

Reynolds stress ~ deformation tensor D_{ij}

<u>Consequence</u>

Stresses are fully correlated with deformation

Stresses are strictly dissipative, $B = 0$, $\varepsilon = P$.

<u>However, this is not true.</u>

$c_B \approx 0.4\text{-}2.4$ (from EDQNM theory)

$B > 0, \ \varepsilon = P - B, B \approx c_B \, \varepsilon$

Simulation of backscatter, e.g., with

- random forces (Mason and Thompson, 1992)
- random stresses R_{ij} (Schumann, 1995)
- nonlinear model (Kosović, 1997)

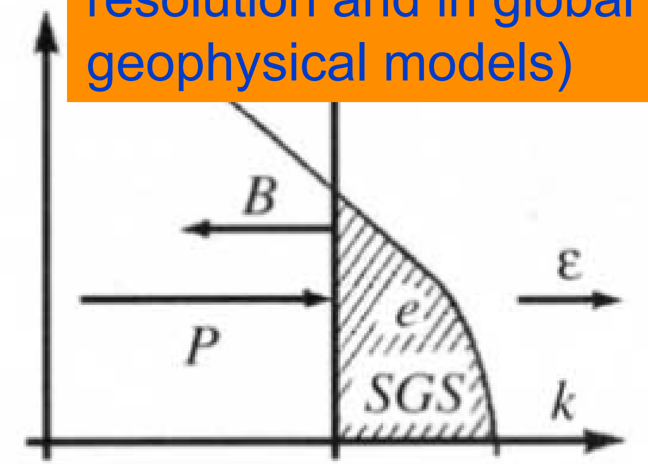

$\overline{u_j}$ $\quad \bar{D}_{ij} = \frac{\partial \bar{u}_i}{\partial x_j} + \frac{\partial \bar{u}_j}{\partial x_i}$ $\quad e = \frac{1}{2}\overline{u_i'^2}$

$$\overline{u_i' u_j'} = -K_m \bar{D}_{ij} + \tfrac{2}{3}\delta_{ij} e$$

$$\overline{u_i' u_j'} = -K_m \bar{D}_{ij} + \tfrac{2}{3}\delta_{ij} e + R_{ij}$$

(Schumann, PRS, 1995)

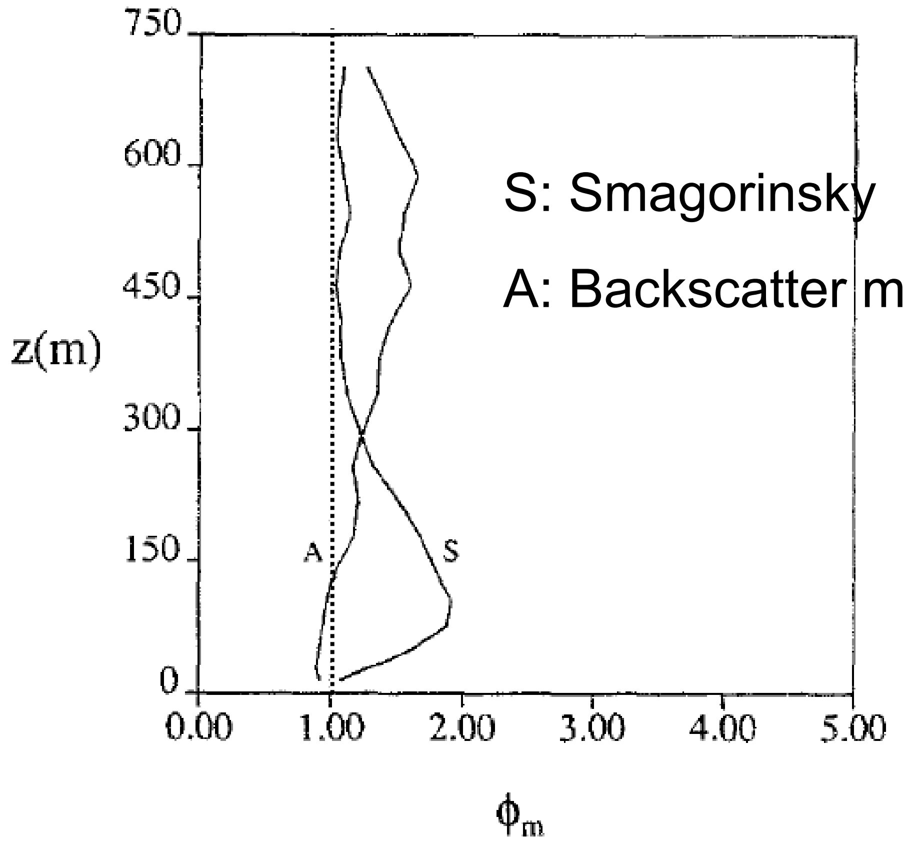

$$\frac{\partial U_s}{\partial z} = \frac{u_* \phi_m}{\kappa z}$$

Fig. 2. Profiles of non-dimensional shear for Smagorinsky run (S) and standard backscatter run (A).

Mason and Brown (BLM, 1994)

Non-linear SGS models (Kosović, JFM, 1997)

$$\sigma_{ij} = -(C_s\Delta)^2 \left\{ 2(2S_{mn}S_{mn})^{1/2}S_{ij} + C_1 \left(S_{ik}S_{kj} - \frac{1}{3} S_{mn}S_{mn}\,\delta_{ij} \right) + C_2 \left(S_{ik}\,\Omega_{kj} - \Omega_{ik}\,S_{kj} \right) \right\}.$$

Simulates backscatter

(stresses σ_{ij} not aligned with deformation S_{ij};

$\varepsilon = -\sigma_{ij} S_{ij}$: not necessarily positive),

reduces mixing in strongly sheared layers,

and is realisable for bounded C_1, C_2

GEWEX Atmospheric Boundary Layer Study:
LES Intercomparison for Weakly Stable Boundary Layer

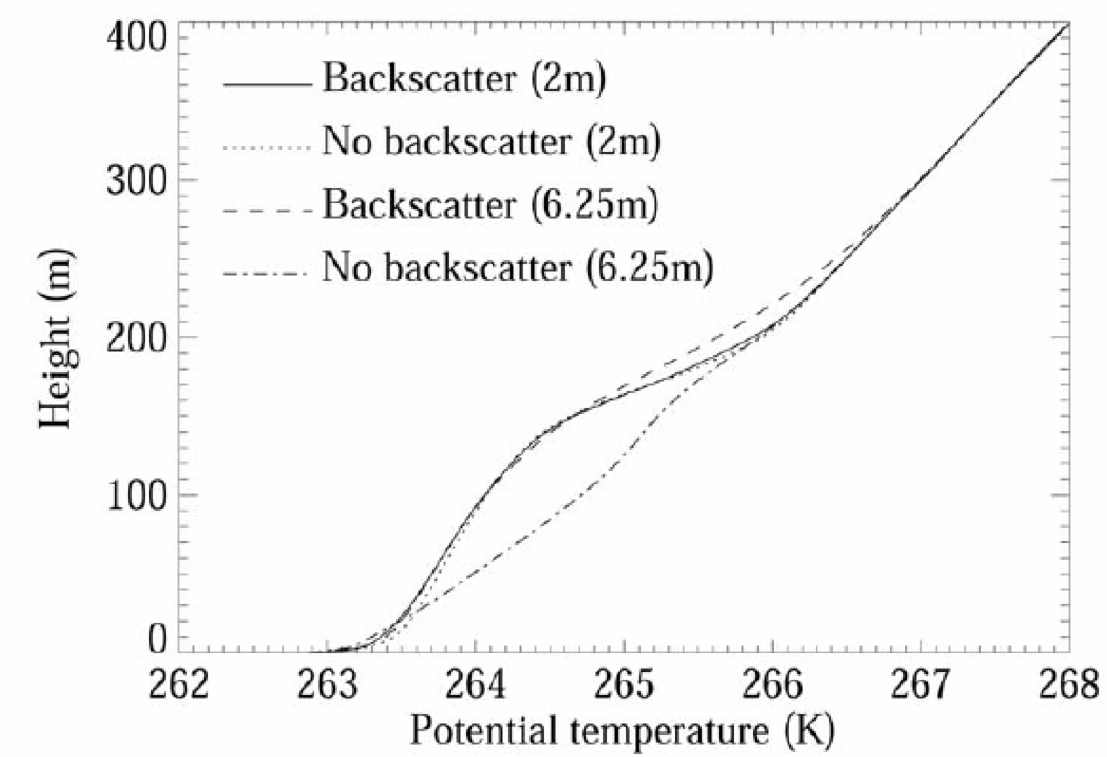

Beare and MacVean (BLM, 2004)

Beare et al. (BLM, 2006):

Sophisticated subgrid-scale models (non-linear, stochastic backscatter, two-part models) are more effective at 6.25-m resolution,

<u>but the results become independent of sub-grid model at 1-m resolution</u>

-> Backscatter and anisotropy are related

The DLR Institute of Atmospheric Physics, Oberpfaffenhofen:

Basis of my research since 1982

The root of the matter is that the greatest stimulus of scientific discovery are its practical applications

L. F. Richardson (1908)

Climate impact of aviation?

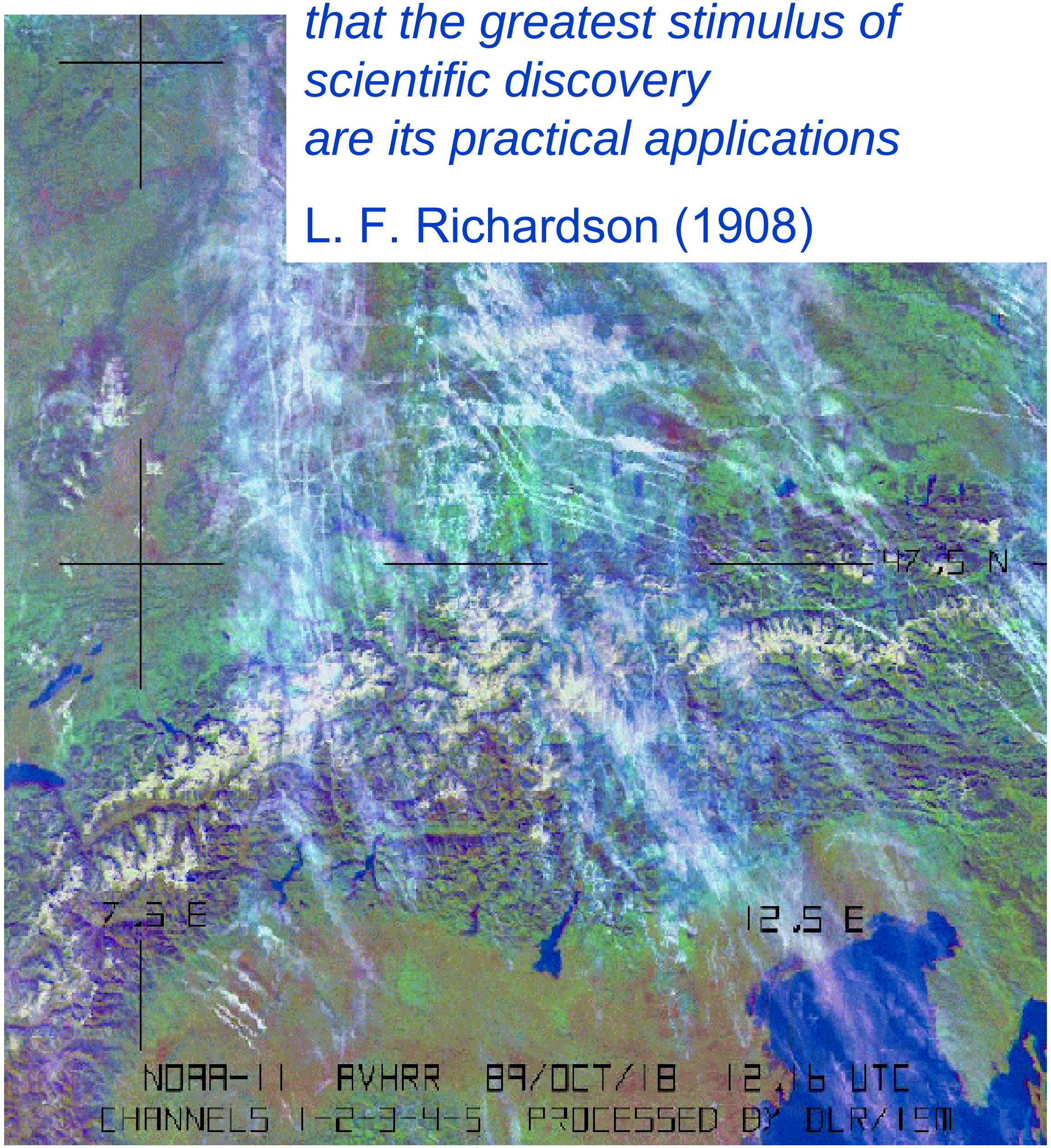

Mannstein et al. (JRS, 1998)

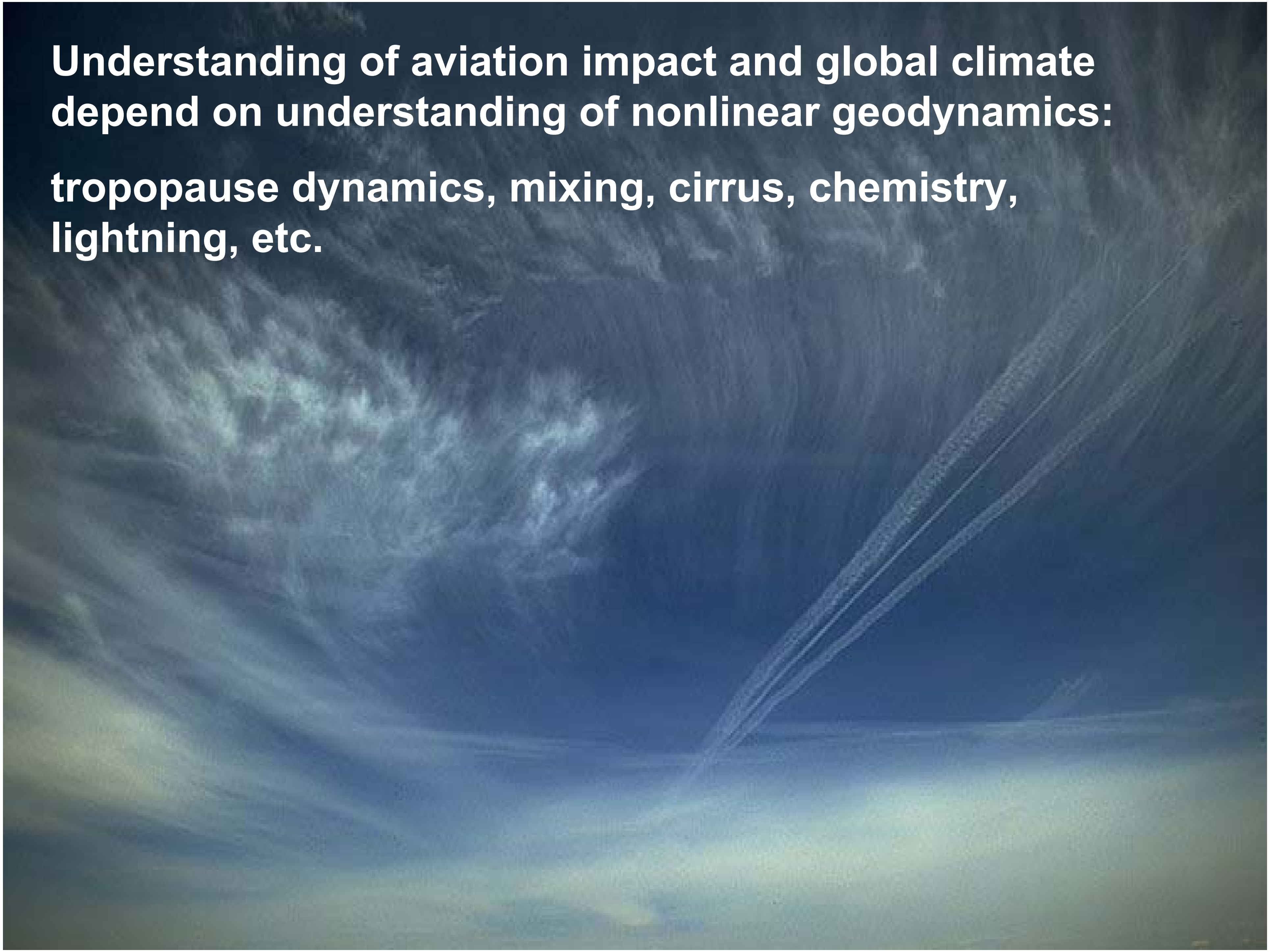
Understanding of aviation impact and global climate depend on understanding of nonlinear geodynamics:
tropopause dynamics, mixing, cirrus, chemistry, lightning, etc.

Experimental determination of aircraft emissions, trace gases, aerosols, contrails

(e.g., Schumann et al., JGR, 1996, 2002)

Measured dilution ratio of trace gases from engine combustion in the wake of aircraft

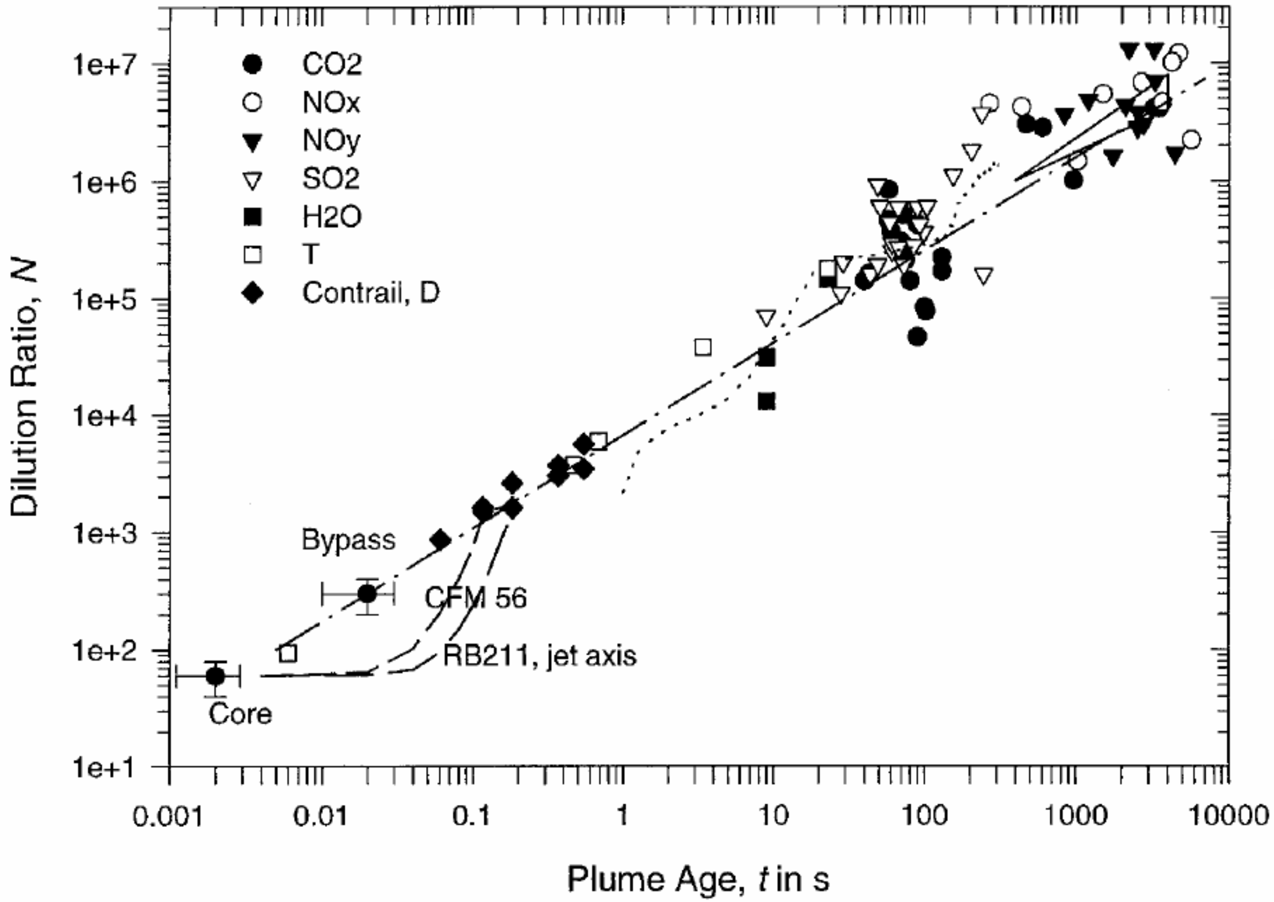

(Schumann et al., AE, 1998)

$$N = \frac{m_{\mathrm{plume}}}{m_{\mathrm{fuel}}}$$

$$\Delta c_i = \frac{\mathrm{EI}_i}{N}$$

$N = N_0\ (t/t_0)^{0.8}$

dilution occurs far slower than in inertial range turbulence

How sharp is the tropopause?

Plot of Stratification (N^2 & θ) from radiosonde data averaged relative to ground

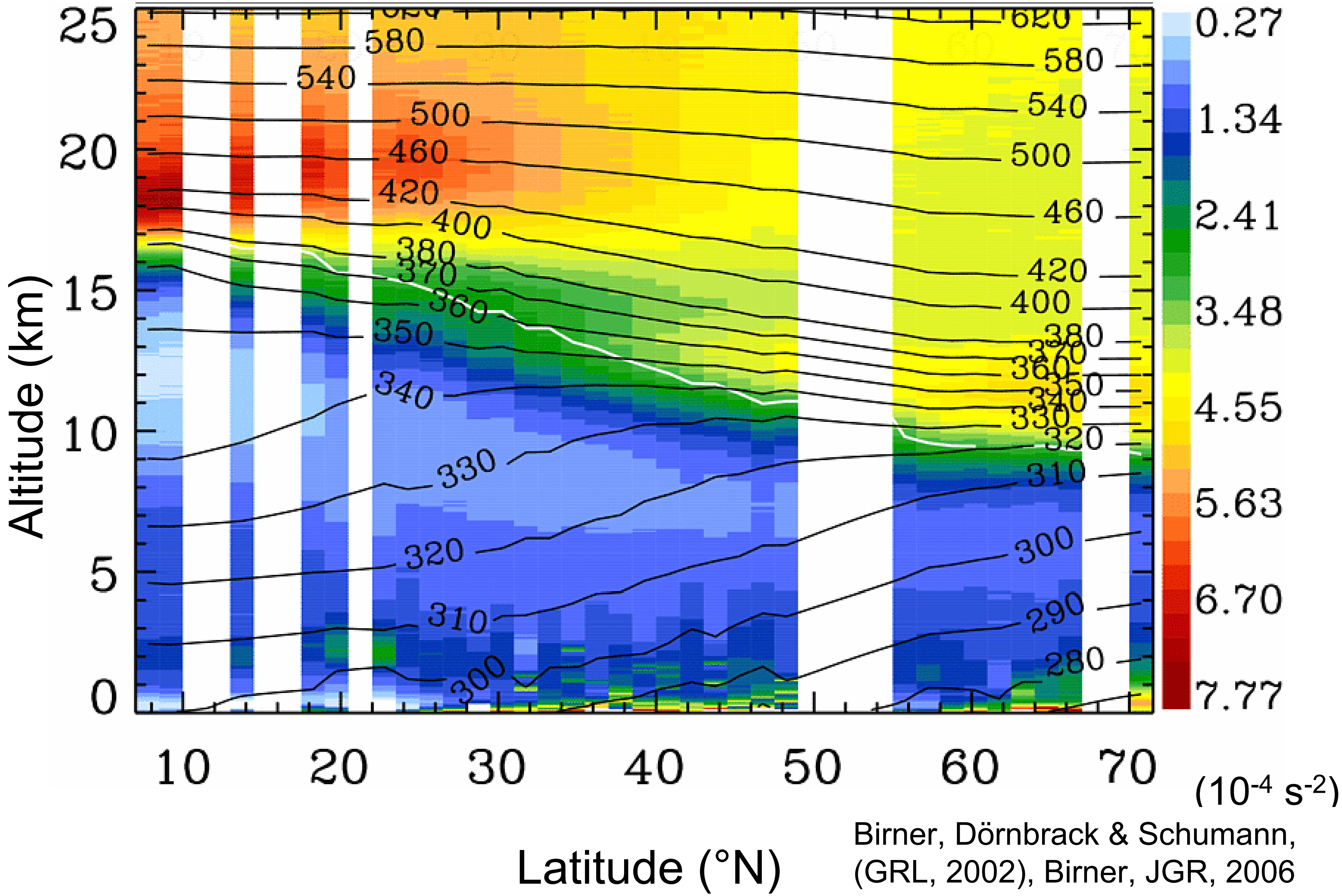

Birner, Dörnbrack & Schumann, (GRL, 2002), Birner, JGR, 2006

How sharp is the tropopause?

Plot of Stratification (N^2 & θ) from radiosonde data averaged relative to TP

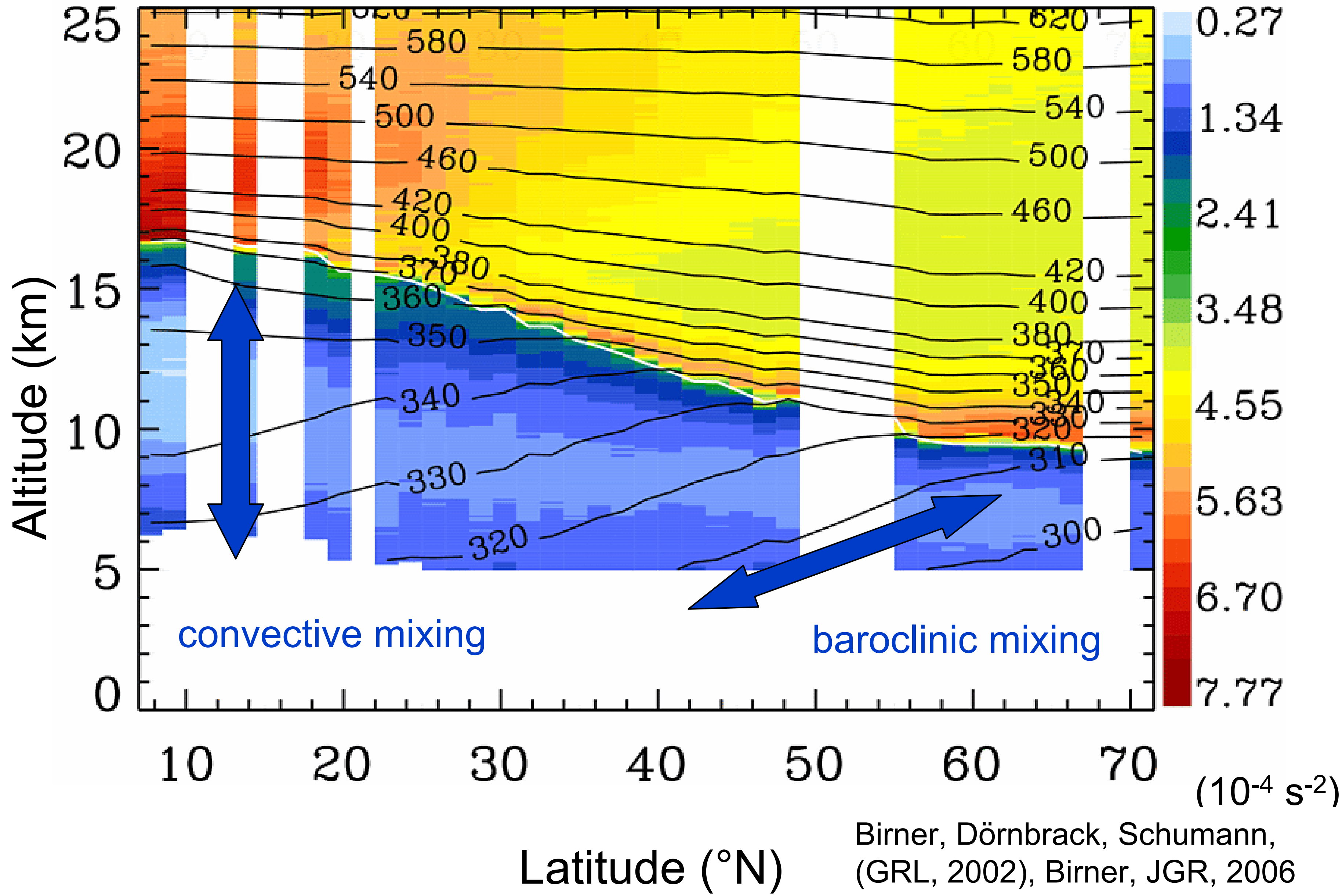

Birner, Dörnbrack, Schumann, (GRL, 2002), Birner, JGR, 2006

Persistent Contrails indicate ice-super-saturation

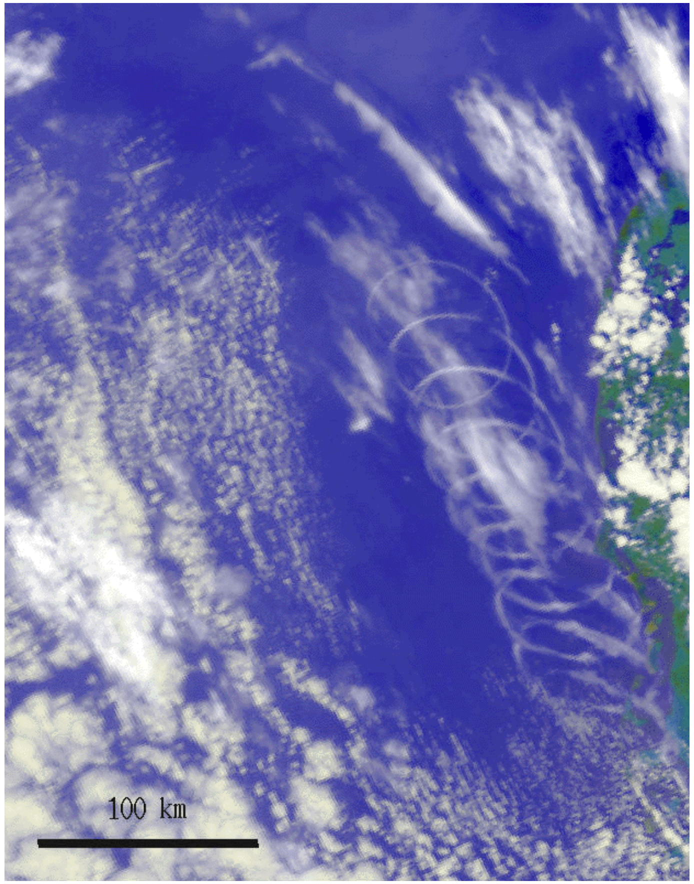

Schumann, 2002

Contrail ~1500 km long,
1.7 - 2 h old.

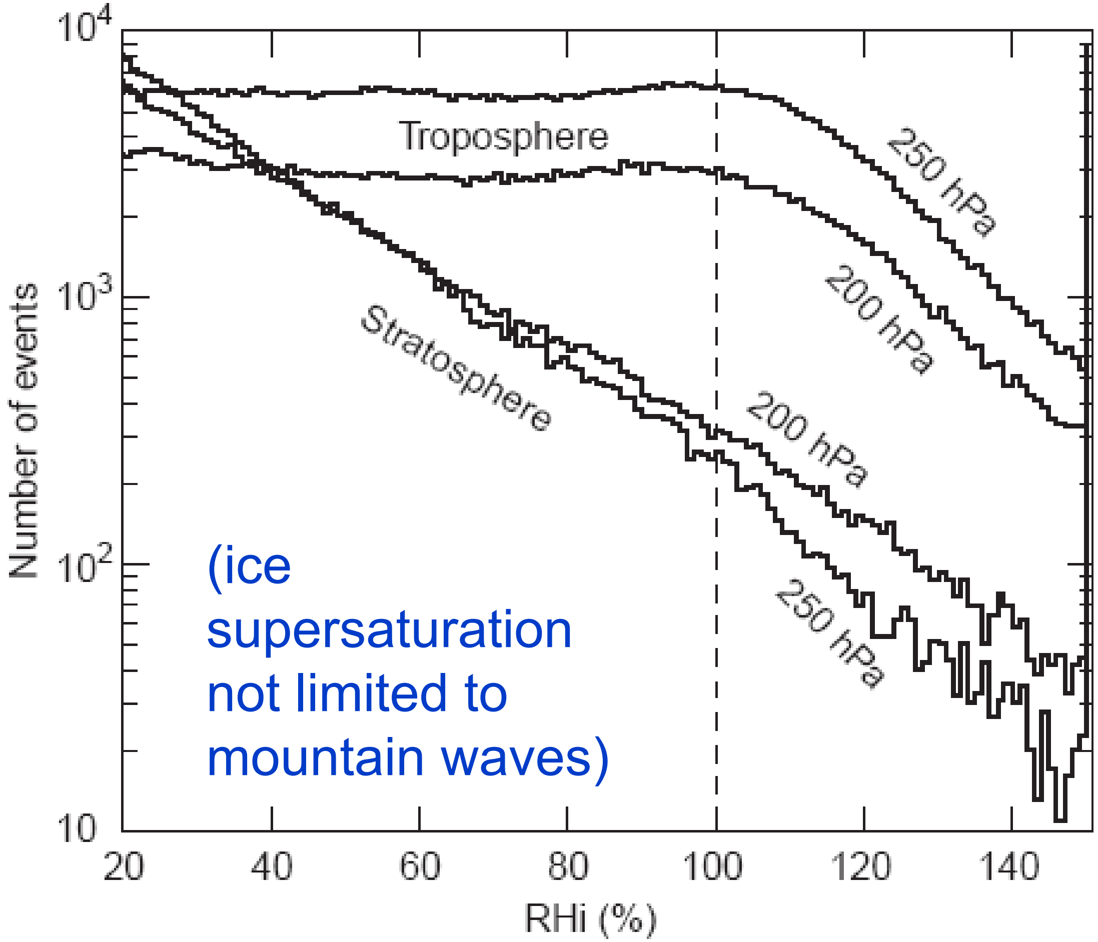

Gierens, Schumann, Helten, Smit, Marenco, (Ann.Geophys., 1999)

Homogenous nucleation limit (Koop et al., 2000; Kärcher and Lohmann, 2002)

Ice saturation

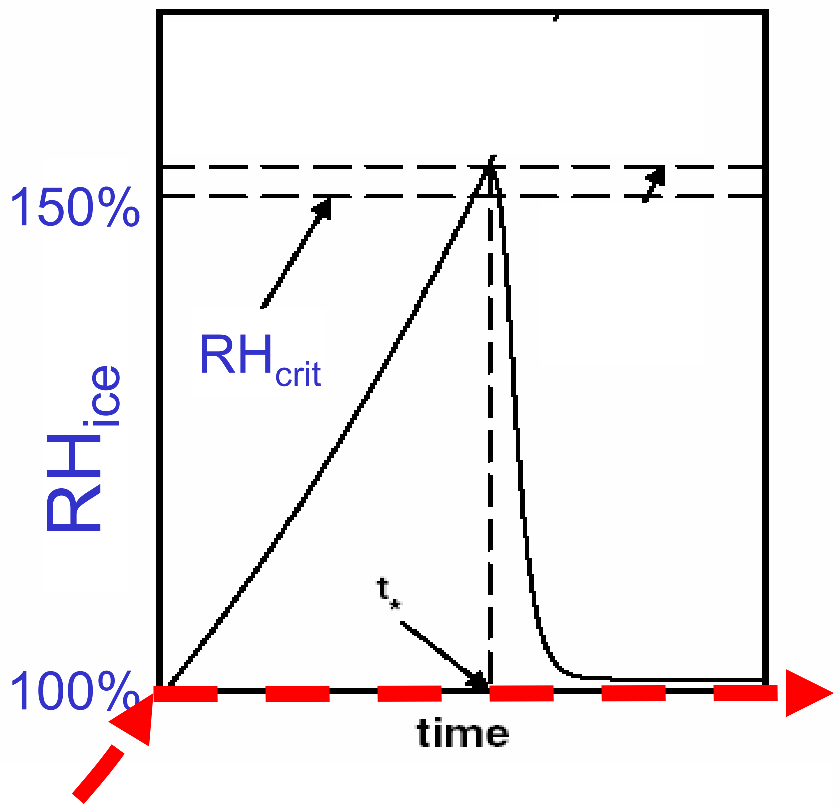

Old approach: no supersaturation

Tompkins, Gierens, Rädel (QJRMS, 2007)

Homogenous nucleation limit (Koop et al., 2000; Kärcher and Lohmann, 2002)

Ice saturation

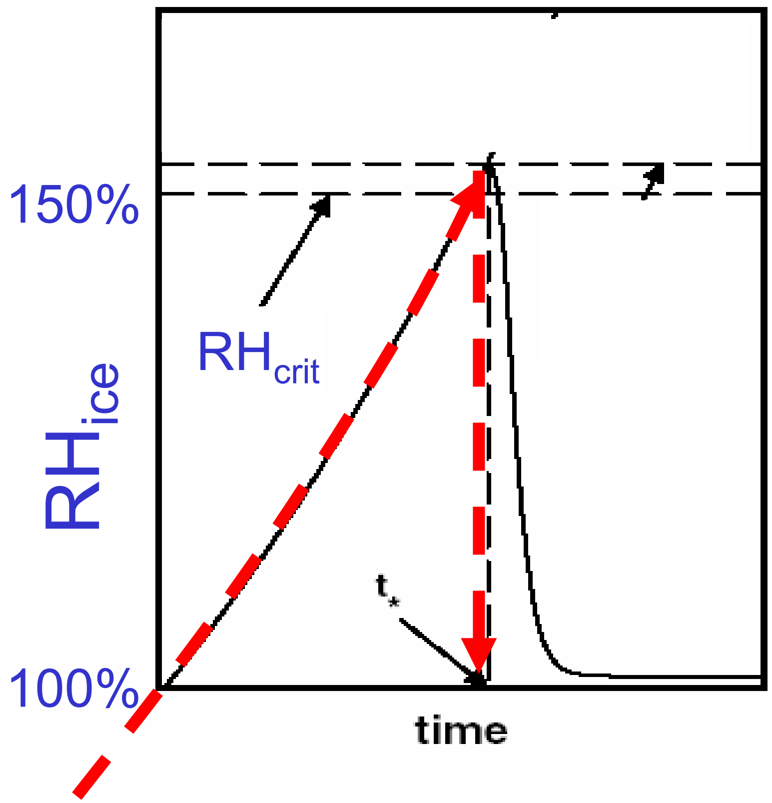

New approach:
homogeneous nucleation threshold for cloud free areas

Tompkins, Gierens, Rädel (QJRMS, 2007)

Ice supersaturation in ECMWF model (since 2006)

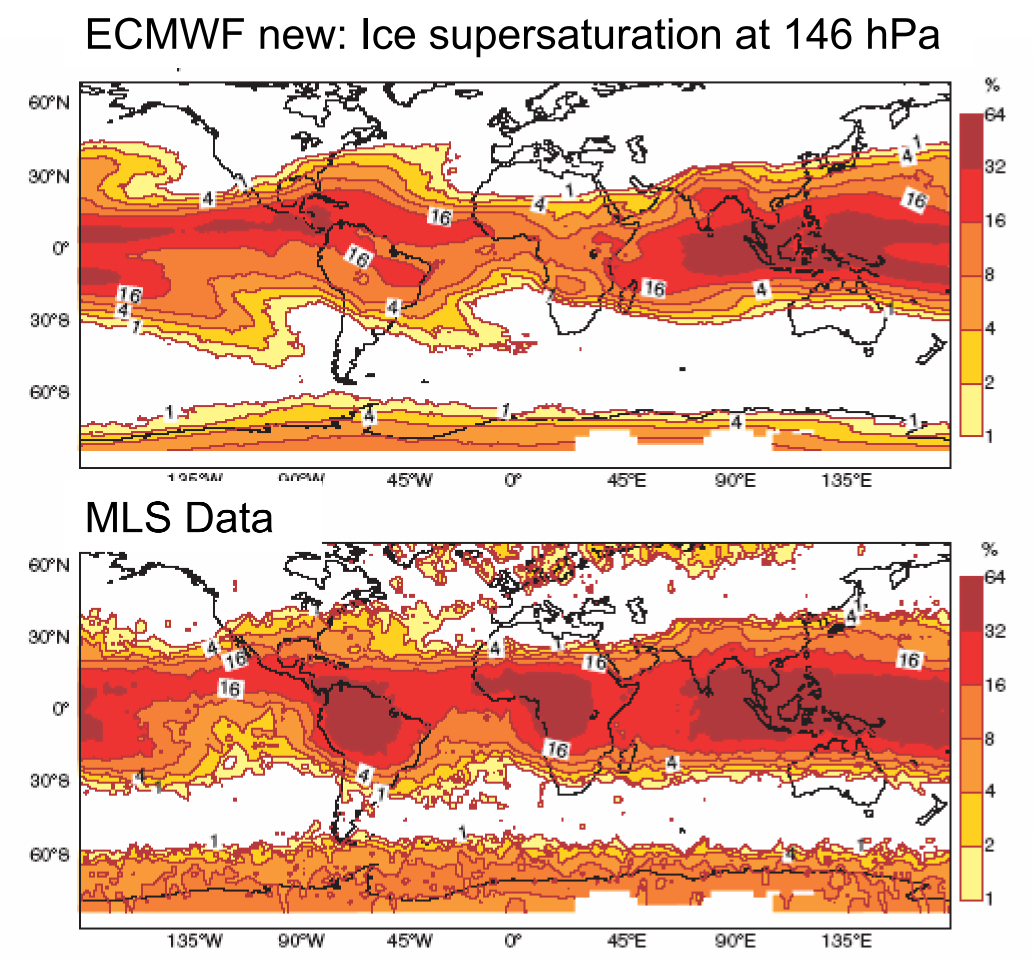

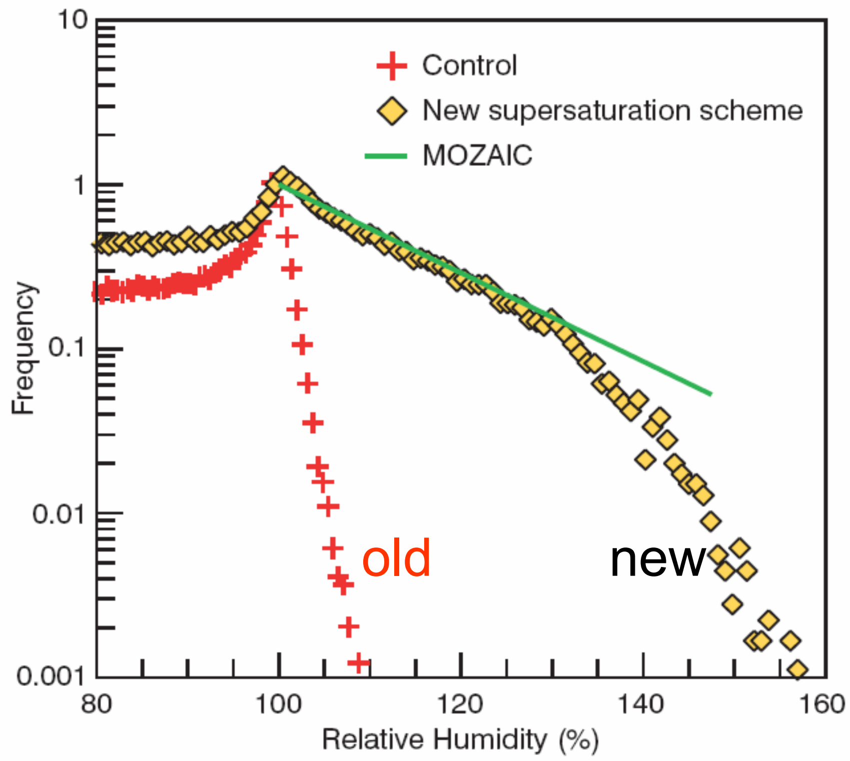

Tompkins, Gierens, Rädel (QJRMS, 2007)

How much NOx is formed from Lightning in Thunderstorms?

(photo taken from Jim Dodge, 2006)

Flash-specific and global LNOx emissions

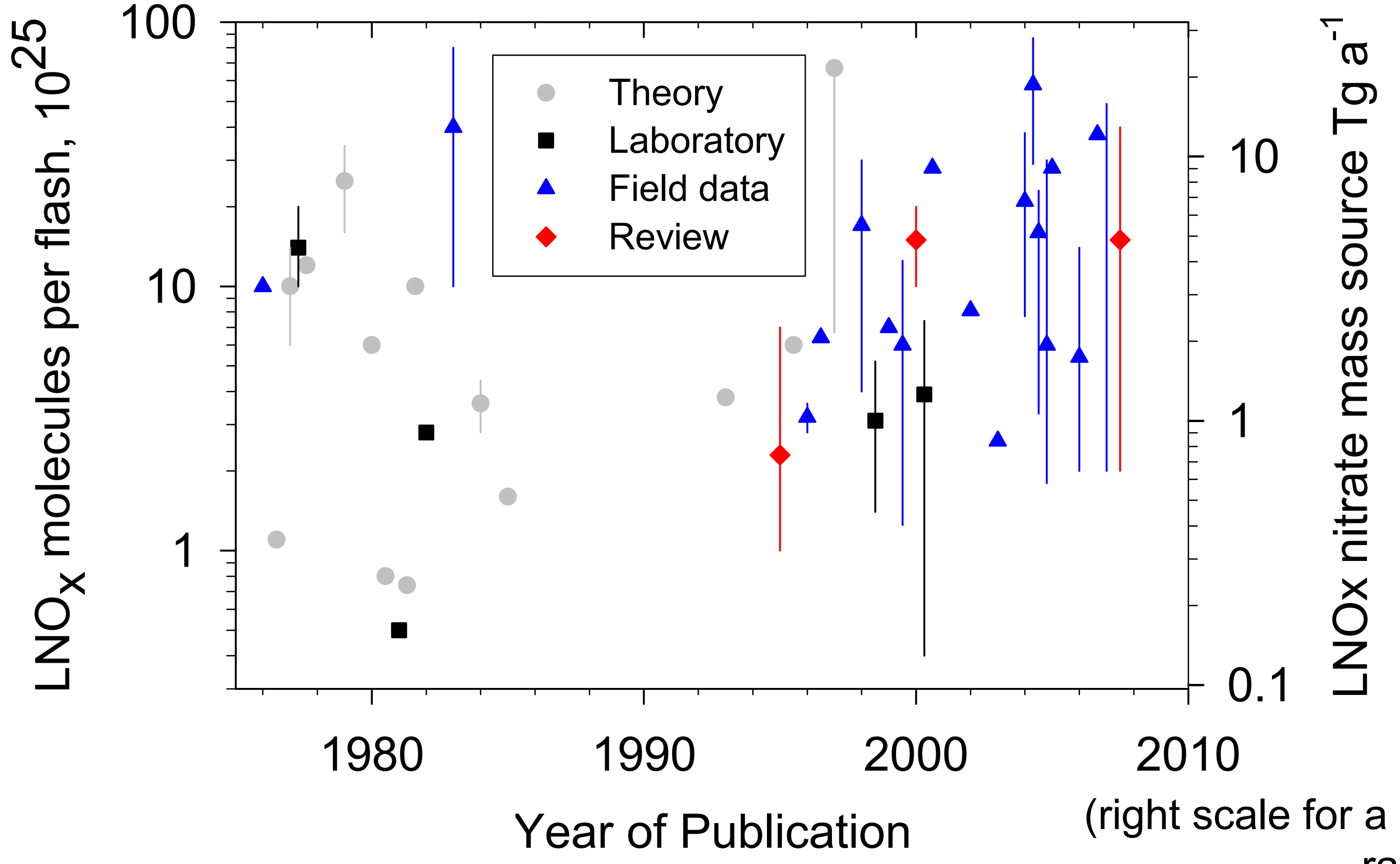

(right scale for a global flash rate of 44 s^{-1})

Required accuracy: 1 Tg/a for reliable prediction of tropospheric chemistry, and climate

Schumann and Huntrieser (2007)

Lightning and the atmospheric composition based on airborne measurements and models

with H. Schlager, H. Höller, H. Huntrieser, R. Sausen, V. Grewe et mult. al.

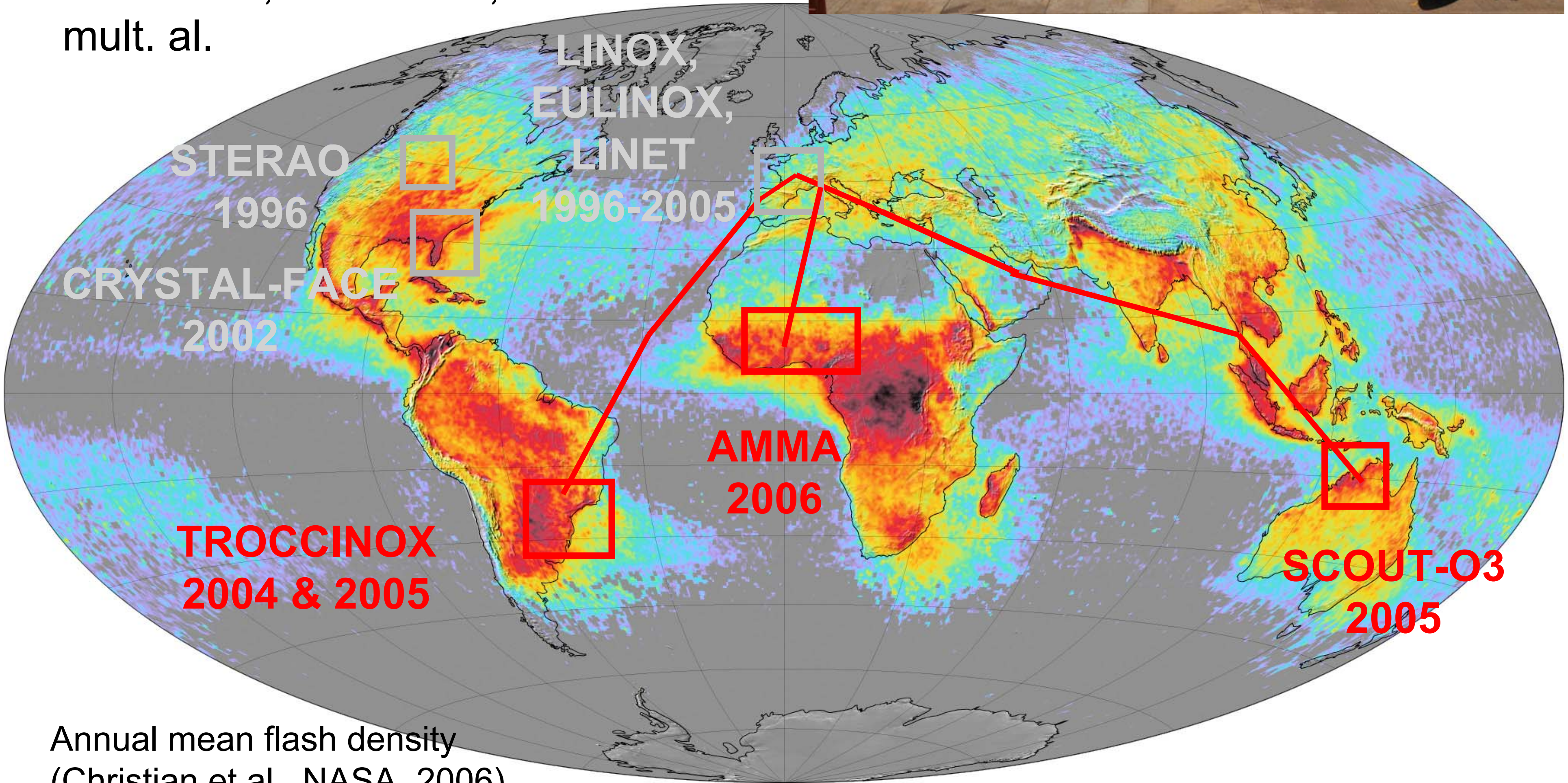

Annual mean flash density (Christian et al., NASA, 2006)

NO, NOy, O_3 and CO from TROCCINOX: LNOx signature

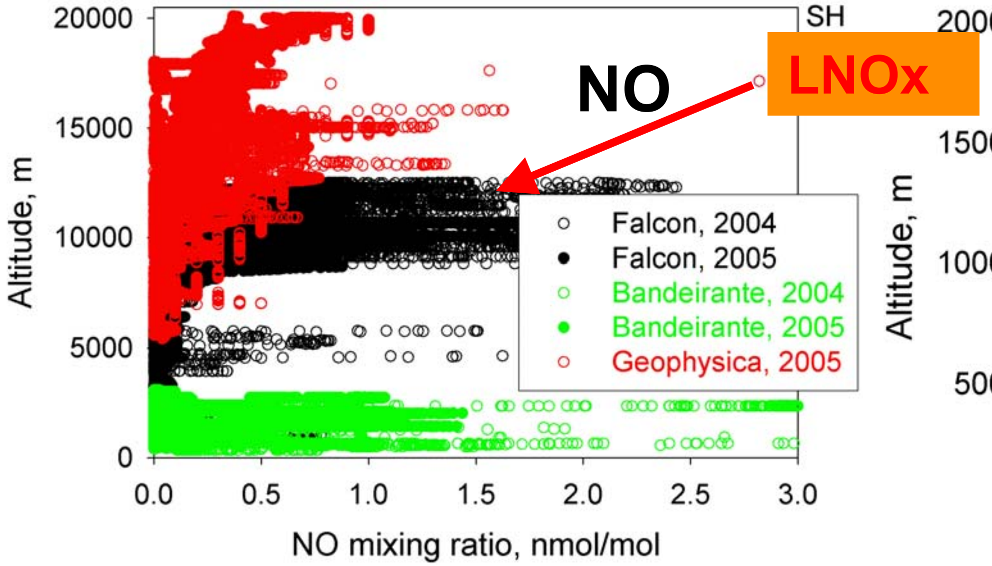

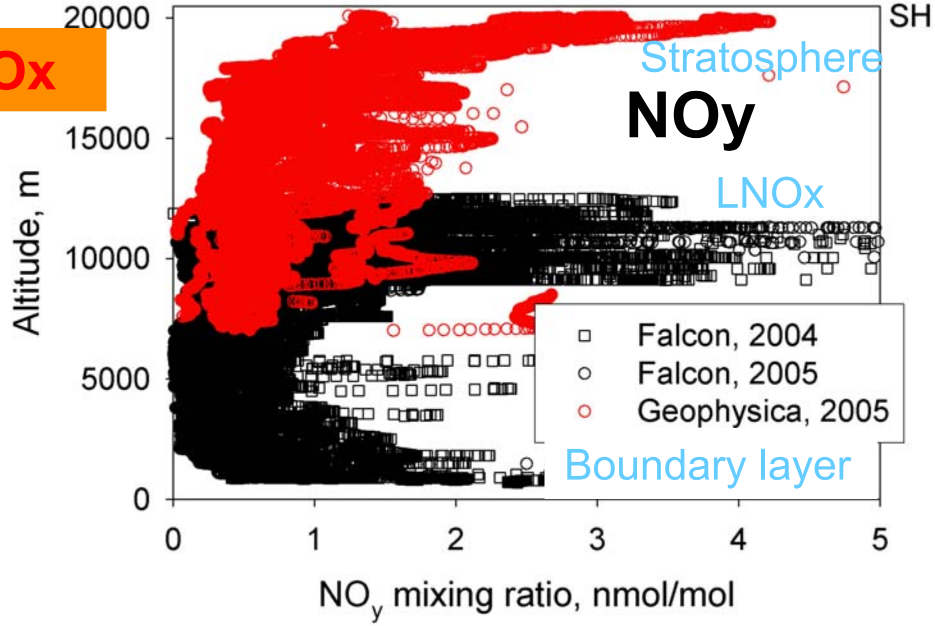

Fit of Chemical-Transport-Model results to measured NOx, O_3, and CO:
global nitrogen LNOx source rate: 5 ± 3 Tg a^{-1}.
(Schumann, Emmons, Kurz, Lawrence, Labrador, Meijer and many others, 2006, and work in progress)

Conclusions

- LES filter is implicit in the grid and discretisation
- SGS model important unless Δ well within Richardson's cascade
- Backscatter important on coarse grids, e.g. in global atmospheric models
- Realizability constraint fundamental for turbulence modelling
- Inversion at tropopause shows *some* similarity to the inversion at top of the convective boundary layer
- Ice-supersaturation, signalled by persistent contrails, now reasonably approximated in ECMWF model. -> allows for contrail/cirrus prediction.
- Lightning induced NOx (LNOx): important for tropospheric chemistry and climate
- (LNOx may increase an order 15 % (5-50 %) per K global warming)
- Present best estimate of LNOx: 5 ± 3 Tg a^{-1}. Required accuracy: 1 Tg a^{-1}
- Combination of global models and measurements in sensitive regions allows to determine critical parameters, such as LNOx source rate
- LES of the global atmosphere with chemistry, still to come